QIRT 10
http://dx.doi.org/10.21611/qirt.2010.056
10th International Conference on Quantitative InfraRed Thermography
July 27-30, 2010, Québec (Canada)

FEATURE-EXTRACTION FROM LOCKIN-THERMOGRAPHY PHASE-IMAGES

by N. Holtmann*, C. Spiessberger*, A. Gleiter*, and G. Busse*

**NDT Dept., Institute for Polymer Technology, University of Stuttgart, 70569 Stuttgart, Germany, niels.holtmann@ikt.uni-stuttgart.de, christian.spiessberger@ikt.uni-stuttgart.de, andreas.gleiter@ikt.uni-stuttgart.de, gerd.busse@ikt.uni-stuttgart.de*

Abstract

The full potential of optically excited lockin-thermography is not used if only one phase image is evaluated. More information can be gained by correlating two or more images. This allows to gather information on features e.g. the kind of defect, thickness of the specimen, properties of boundary layers, or lateral heat flow. Certain defects are correlated to specific patterns in a scatterplot, akin to a fingerprint. Specimens with and without a certain feature can be distinguished more easily using suitable filters. This is apparently of interest for automated defect detection.

This paper deals with qualitative feature-extraction using scatterplots and outlines the potential for quantitative evaluation.

1. Introduction

The correlation or data fusion of two different NDT-methods can provide more information than just one measurement [1-4]. This holds true not only for different NDT-methods, but also for two or more different lockin-frequencies within one method [5,6]. Certainly correlation does not generate new data, but presents it in a new way, thereby revealing new aspects or even discernable patterns. To visualize hidden patterns with multiple phase-images we use scatterplots where two or more phase-angle images are pixelwise plotted against each other. The dimension and thereby the complexity of a scatterplot grows with the number of phase-images you want to correlate. For reasons of perceptibility, this paper covers only two dimensional correlation.

2. Theory

The complex amplitude of a thermal wave at the surface of a flat sample consisting of one layer with thickness L and a thermally infinite substrate is [7,8]

$$\theta(L, f) = \frac{F_0}{4k\sigma}\left(\frac{\left(1+R_1\right)\left(1+R_2 e^{-2\sigma L}\right)}{1-R_1 R_2 e^{-2\sigma L}}\right) \tag{1}$$

where F_0 is a constant, k the thermal conductivity, R the thermal wave reflection coefficient of the rear sample surface, and σ the complex wave number linked to the thermal diffusion length μ by

$$\sigma = \frac{1+i}{\mu} = \left(1+i\right)\sqrt{\frac{\pi f}{\alpha}}\,, \tag{2}$$

with the modulation frequency f and thermal diffusivity α. The reflection coefficient R depends on the effusivities of the materials on both sides of the interface measured:

$$R = \frac{e_1 - e_2}{e_1 + e_2} \tag{3}$$

The phase value can be extracted from Eq. (1) using

http://dx.doi.org/10.21611/qirt.2010.056
10th International Conference on Quantitative InfraRed Thermography

$$\Phi = \arg\big(\theta(L, f)\big). \tag{4}$$

The phase has a characteristic dependence on sample thickness where frequency is a parameter (figure 1) [9].

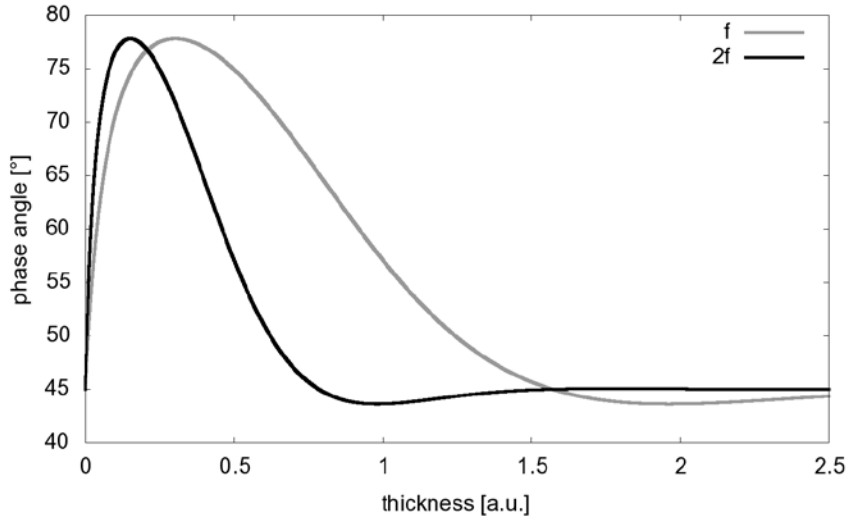

Fig. 1. *Phase angle in respect of thickness, plotted for two lockin-frequencies, one twice as high as the other*

The reflection coefficient R at the measured boundaries significantly affects the phase contrast of lockin thermography. For the boundary solid / air R is almost 1, and almost –1 when the thermal wave in a thermally insulating material hits a boundary to a good thermal conductor (e.g. from polymer to aluminium). When R is close to zero the thermal wave is not reflected at all. The dependence of the phase curve on the reflection coefficient is plotted in figure 2 [10]. In combination with figure 1, this shows an only ambiguous link to the thermal thickness (figure 1) and reflection coefficient (figure 2) for a phase angle calculated at only one lockin-frequency.

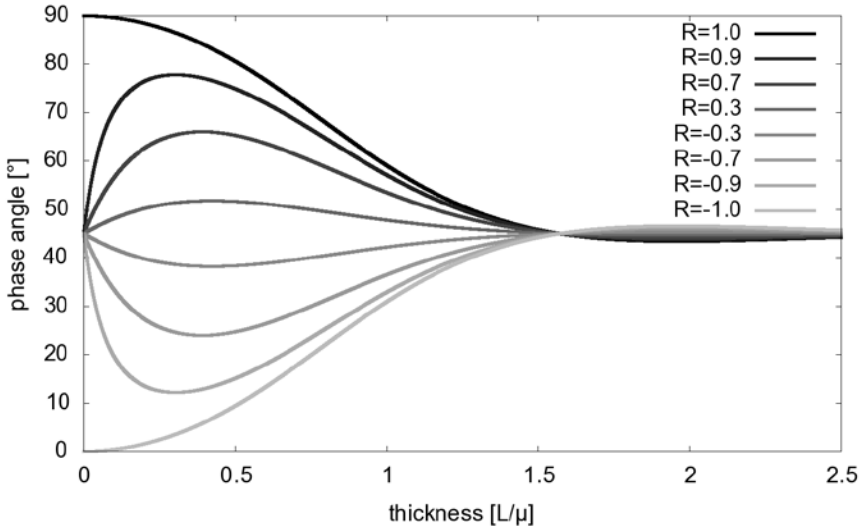

Fig. 2. *Phase depending on thickness and reflection coefficient R ranging from 1 to -1* [10].

http://dx.doi.org/10.21611/qirt.2010.056

It is therefore beneficial to combine two or more measurements in one diagramm, e.g. in a two- or multi-dimensional scatterplot. Figure 3 shows such a correlation of two phase angle curves as in figure 1, plotted against each other. Each pair of initial phase angle curves leads to an oval shaped curve in a scatterplot. Smaller reflection coefficients result in a reduced size of the oval. It is thereby possible to determine the reflection coefficient of a specimen of varying thickness, as for example a wedge.

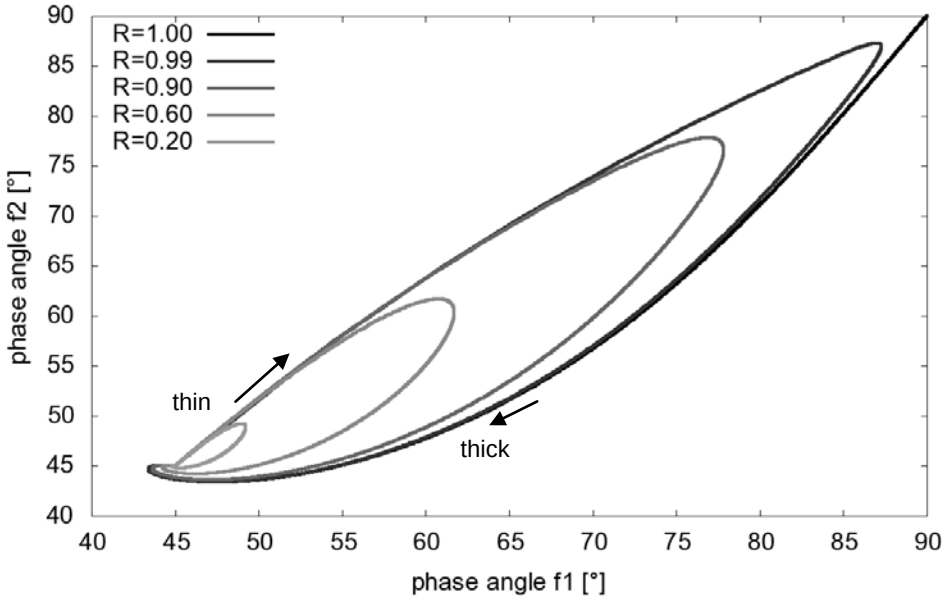

Fig. 3. *Phase angle scatterplot for 1d for reflection coefficients ranging from 0.2 to 1. Parameter of each curve is plate thickness [5].*

3. Mapping lateral heat flows

The heat flow within a specimen is generally three dimensional. Figure 4 indicates which direction is meant in the following by a one-(respectively two- and three-) dimensional approach. The one-dimensional theory used to this point does exclusively cover the heat flow in direction 1, as given by equation 1 for local thickness L. Actual measurements, however, are influenced by additional heat flows in the lateral directions 2 and 3, which affect the measured phase angle.

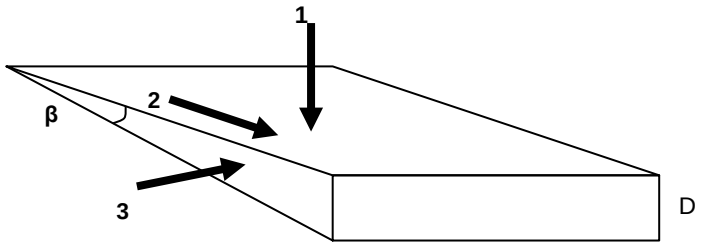

Fig. 4. *Wedge with indicated directions of heat flow.*

The analytic curve in figure 5 is based on the assumption of a wedge with only one-dimensional heat flow (using equations 1 and 4), whereas the simulated curves include the second dimension of heat flow as well (see figure 4 for reference). This lateral heat flow is driven by an accumulation of heat in thin areas. As expected, the difference in figure 5 is only visible at small thicknesses, where the impact of lateral heat flows is strongest. According to this effect the phenomenon is stronger for steeper wedges having larger β.

http://dx.doi.org/10.21611/qirt.2010.056
10th International Conference on Quantitative InfraRed Thermography

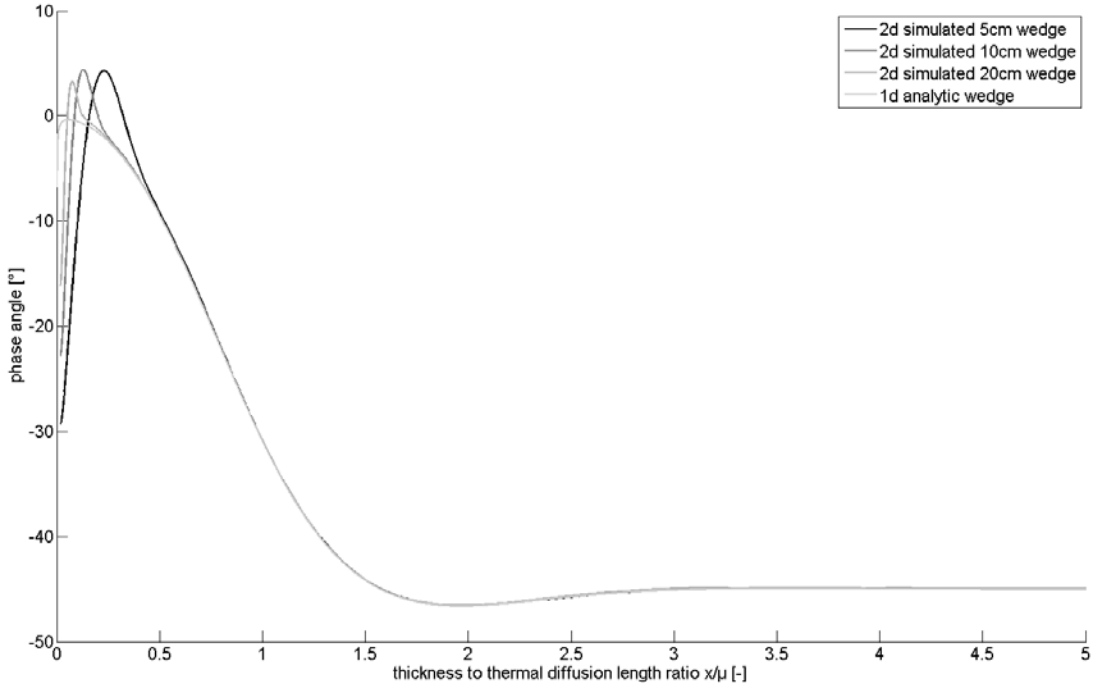

Fig. 5. *Phase in respect of thermal thickness for one- (respectively two-) dimensional heat flows and wedges with 3 different lengths at the same thickness, hence 3 values of β.*

These deviations from the one-dimensional simplification are clearer in a scatterplot (figure 6). Both 1d-theory and 2d-simulation are unaffected by convection, heat radiation or other disturbances. Differences can therefore only occur due to lateral heat flows whose influence was varied by the geometry of the simulated wedges. The thickness D of the 2d-specimens remained unchanged, while the length was varied, effectively changing the angle β of the wedge, see figure 4.

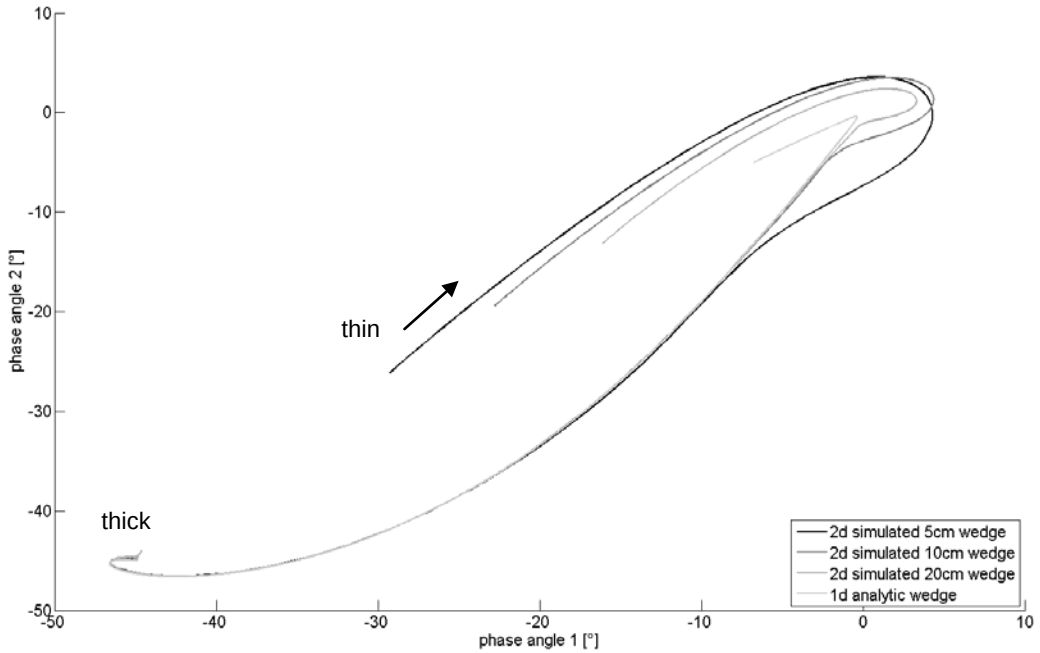

Fig. 6. *Phase angle scatterplots for 1- and 2-dimensional heat flow in wedges. Parameter is local thickness L.*

As expected, the impact of lateral heat flows is maximal for the shortest wedge and extends to greater thicknesses than for the longer wedges. Using suitable filters, this can be traced back to certain regions of the specimen, thereby highlighting the areas where the phase angle is affected by lateral heat flows.

The simulation is confirmed by measurements on an epoxy wedge, cast on an aluminium substrate (figure 7), which results in a reflection coefficient of nearly 1 at the air/epoxy boundary and a reflection coefficient of nearly -1 at the epoxy/aluminium boundary.

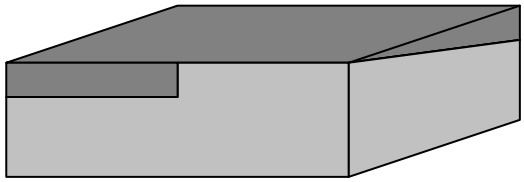

Fig. 7. *Epoxy/aluminium sample with wedged area*

The dashed rectangular areas in the corresponding phase images (figure 8) were correlated in a scatterplot (figure 9).

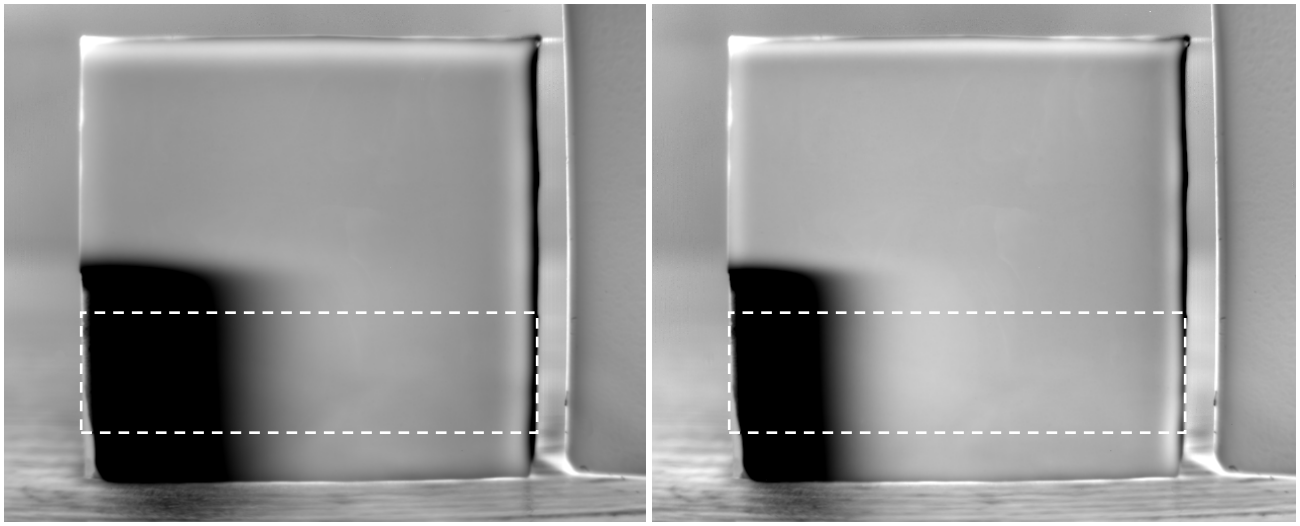

Fig. 8. *Phase images of the epoxy/aluminium sample at two different lockin-frequencies*

http://dx.doi.org/10.21611/qirt.2010.056
10th International Conference on Quantitative InfraRed Thermography

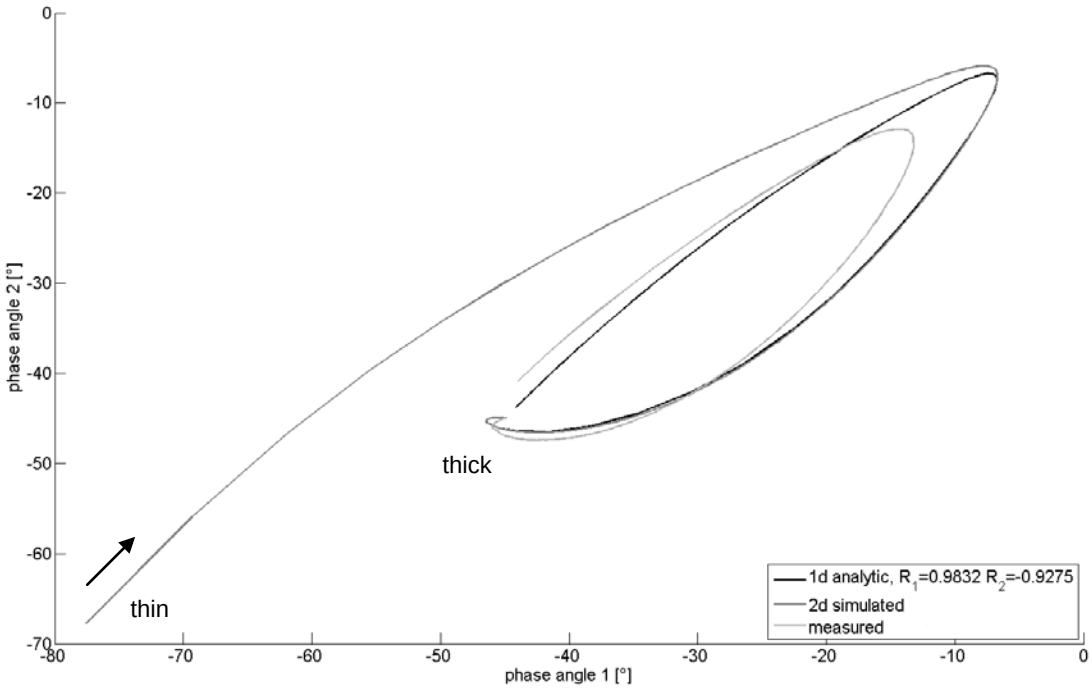

Fig. 9. *Phase angle scatterplots for 1-, 2- and 3-dimensional heat flow in a wedge*

The measured data deviates from the calculated curves, which is due to a combination of several effects. Some of these are lateral heat flows, convection, heat radiation and the quality of bonding between the epoxy and aluminium. The latter effect is presumably the easiest to extract, as figure 9 shows the characteristics of a lower reflection coefficient (see figure 3 for reference) than the calculated curves. Additionally the measured curve shows a distinctive feature at the thinnest end, differing from the 1d-curve in the direction of the 2d-curve, which indicates lateral heat flows in that particular area.

Tracing these discrepancies back to the original phase image highlights the areas where they belong to (figure 10). These areas would lead to incorrect calculations of reflection coefficient or thickness, which are based on the 1d-theory. The tool of backtracing lateral heat flows to their location, as shown in this paper, allows to identify and eliminate the affected areas for quantitative evaluation.

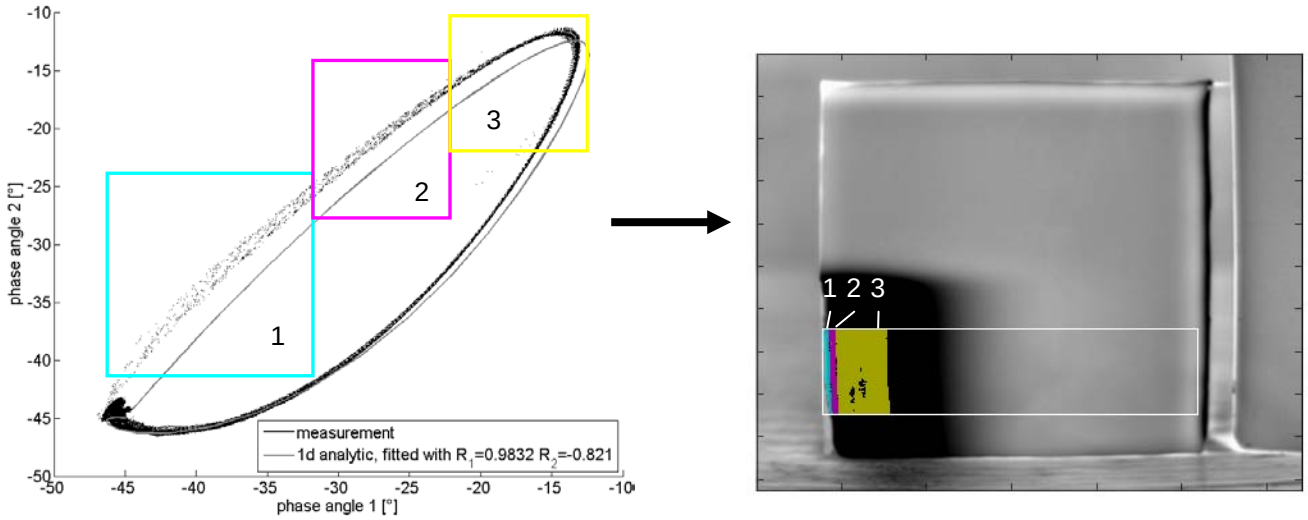

Fig. 10. Phase angle scatterplot (left) and three different areas traced back to their origin in the phase image (right)

4. Conclusion

We have shown a data-fusion approach to access different features which can otherwise not be extracted from measurements. The basic idea is to correlate two or more phase angle images e.g. into a scatterplot: Certain patterns are discernible in a scatterplot but not in a single phase image. The deviation from the 1 dimensional theory to 2 dimensional heat flow (as described for edge effects [15]) should – as a fingerprint of lateral heat flows – be detectable in all measurements, when they are evaluated as a scatterplot. Detecting or mapping the lateral heat flows is important to avoid incorrect calculations of features like reflection coefficients or thicknesses. Future investigations will deal with other features, such as certain defects or quantitative thicknesses.

REFERENCES

[1] L. Diener, P. Elsner, M. Ota, G. Busse, B. Brühl: Neuere Methoden der zerstörungsfreien Prüfung für Polymerwerkstoffe. Berlin: DVM, p. 261-276, 1990.
[2] K. Tsukada, K. Hanasaki, X.E. Gros, Z. Liu: Experimenting with pixel level NDT data fusion techniques. IEEE Trans. Instrum. Meas., 49(5):1083-1090, 2000
[3] G. Busse: Hybride Verfahren in der Zerstörungsfreien Prüfung (ZfP): Prinzip und Anwendungsbeispiele. In O.W. Geisler O.W. Buchholz, eds., Herausforderung durch den industriellen Fortschritt. Publisher: Stahleisen GmbH, Düsseldorf, 2003.
[4] J.P. Komorowski, K. Hanasaki, T. Kirubarajan, Z. Liu, D.S. Forsyth: Survey: State of the Art in NDE data fusion techniques. IEEE Transactions of Instrumentation and Measurement, 56, p. 2435-2451, 2007
[5] C. Spiessberger, A. Gleiter, G. Busse: Merkmalsextraktion und Defektklassifizierung mit Lockin-Thermografie. MP Materials Testing 50, p. 632-639, 2008
[6] C. Spiessberger, A. Gleiter, G. Busse: Data fusion of lockin-thermography phase images. Quantitative InfraRed Thermography Journal 6, in print, 2009
[7] J. Jaarinen: Nondestructive Evaluation of Coatings by Low-Frequency Thermal Waves, Acta Polytechnica Scandinavica, Applied Physics Series No.162, 1988
[8] A. Mandelis: Diffusion-Wave Fields, Springer, 2001
[9] G. Busse: Phase angle measurement for probing a metal, Appl. Phys. Lett. vol. 35, 1979, p. 759-760.
[10] C.A. Bennett, R.R. Patty: Thermal wave interferometry: A potential application of the photoacoustic effect, Applied Optics 21, p. 49-54, 1982
[11] G.M. Carlomagno, P.G. Berardi: Unsteady thermography in nondestructive testing. Proceedings of the 3rd Biannual Information Exchange, St. Louis/USA, p. 33-39, 1976
[12] J. L. Beaudoin, E. Merienne, R. Danjoux, M. Egee: Numerical system for infrared scanners and application to the subsurface control of materials by photo-thermal radiometry. Infrared technology and applications. SPIE 590, p. 287, 1985
[13] P. K. Kuo, Z. J. Feng, T. Ahmed, L. D. Favro, R. L. Thomas, J. Hartikainen: Parallel thermal wave imaging using a vector lockin video technique. In: Photoacoustic and photothermal phenomena (P. Hess und J. Pelzl, eds.), Springer, Heidelberg, p. 415-418, 1988
[14] G. Busse, D. Wu, W. Karpen: Thermal wave imaging with phase sensitive modulated thermography. J. Appl. Phys. 71 8, p. 3962-3965, 1992
[15] Aamodt, L. C., Murphy, J. C.: Effect of 3-D heat flow near edges in photothermal measurements. Appl. Opt. 21, p. 111-115, 1982